Crossover from reptation to Rouse dynamics in the extended Rubinstein-Duke model

Andrzej Drzewiński
Institute of Physics, University of Zielona Góra, Prof. Z. Szafrana 4a, 65-516, Zielona Góra, Poland

J. M. J. van Leeuwen
Instituut-Lorentz, University of Leiden, P.O. Box 9506, 2300 RA Leiden, The Netherlands
(Received 21 November 2007; published 13 March 2008)

The competition between reptation and Rouse dynamics is incorporated in the Rubinstein-Duke model for polymer motion by extending it with sideways motions, which cross barriers and create or annihilate hernias. Using the density-matrix renormalization-group method as a solver of the master equation, the renewal time and the diffusion coefficient are calculated as functions of the length of the chain and the strength of the sideways motion. These types of moves have a strong and delicate influence on the asymptotic behavior of long polymers. The effects are analyzed as functions of the chain length in terms of effective exponents and crossover scaling functions.

DOI: 10.1103/PhysRevE.77.031802 PACS number(s): 61.25.hk, 05.10.−a, 83.10.Kn

I. INTRODUCTION

A dilute solution of linear polymers in a gel provides the ideal case for reptation. The gel is a rigid network of obstacles which forces the polymer to find its way by slithering through the maze. Effectively, the polymer moves inside a tube of pores which changes only by growing and shrinking at the ends of the tube. It is not a great step to replace the network of the gel by a regular lattice. The regularity of the lattice still keeps the motion of the polymer random, because the ends randomly leave or enter cells of the lattice. A big step is the reduction of the motion to a stochastic process of hopping units. It certainly cannot be justified on the level of monomers, because neighboring monomers are strongly correlated in their motion. For this purpose the notion of reptons has been introduced: blobs of monomers of the size of the correlation length [1]. Seeing the polymer as a sequence of reptons permits the units of motion to be considered as uncorrelated, with the only proviso that they do not separate too far, in order to preserve the integrity of the polymer.

Rubinstein [2] designed an elementary model for reptation, as a chain of slack and taut links connecting the reptons. A slack link describes two successive reptons in the same cell and a taut link two in nearest neighbor cells. By allowing only these configurations of reptons and only moves between them, a simple model for reptation results. Duke [3] enriched the model by biasing the hopping of reptons by an external field, thus modeling the experimental situation of gel electrophoresis. Of course, the model misses important aspects of polymer dynamics, such as the hydrodynamic interactions and even more importantly the requirement of self-avoidance, which influences the universal properties [4,5]. One can incorporate self-avoidance in the model, which, however, makes the analysis an order of magnitude more difficult. An excuse for leaving out this aspect is that mutual exclusion is less severe for reptons than for monomers, because the reptons are loosely packed blobs of monomers which can interpenetrate each other.

The eternal dilemma is to choose between being realistic and keeping the model simple. The chemical culture opts for being realistic and deals with specific properties; the physical culture leans toward simplicity and aims at generic properties. It was de Gennes' contribution to polymer physics to show that properties of long polymers do not depend on the specific composition; in particular, the dependence on the length of the polymers is governed by universal exponents. In this sense the Rubinstein-Duke (RD) model has been shown to catch the essential physics of reptation in spite of the crude approximations made.

We will approach the problem from the physical perspective and deal with the universal properties of the RD model, but investigate a richer class of motions than treated so far. In the standard RD model only interchange of slack and taut links is permitted. This means that the length stored in a slack link moves in the direction of a taut link, interchanging the slack and taut links. A move that would perfectly fit in the spirit of the RD model is the change of two consecutive slack links into two taut links. It corresponds to three reptons in the same cell, of which the middle one escapes to a neighboring cell. Such a move does not cross a barrier. There was a practical reason to exclude this possibility, because it destroys the dimensional reduction, as was pointed out by Duke. From a physical point of view, the formation of "hernias" does not seem to influence the universal properties, and in this paper we investigate this issue. Another optional move is the interchange of two taut links. As we will see, this means the crossing of a barrier by the chain. If the barriers posed by the obstacles were infinitely high, these processes would be strictly forbidden. But barriers are not perfect and therefore it is worthwhile to investigate the influence of finite barriers. Moreover, we will see that barrier crossing in the RD model does not lead to much change, but the combination with hernia creation and annihilation has the drastic effect of crossing over from reptation to Rouse dynamics.

Since the standard RD model already does not permit an exact solution, we have to rely on numerical methods to analyze the extended model. The most common method is simulation of the system but this is less suited for our goal, because the crossover between the two types of dynamics occurs for rather long chains, which are hard to simulate accurately. We will employ the technique of finite-size analysis, which requires very accurate data to be successful. In this

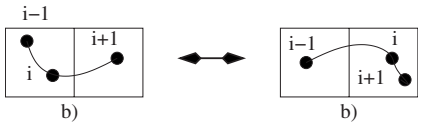

FIG. 1. Rubinstein-Duke moves. Their rate is set to 1.

paper we use a method, based on the analogy between the master equation and the Schrödinger equation, by which the temporal evolution of the probability distribution of the chain configurations corresponds to the evolution of the wave function. The master operator corresponds to the Hamiltonian of a one-dimensional spin chain, for which the very efficient density-matrix renormalization-group method (DMRG) has been designed by White [6]. The model remains a one-dimensional quantum problem, irrespective of the lattice in which it is embedded, because the chain itself is a linear structure. Application of the DMRG method to the chain dynamics on a lattice is by now standard, but to perform calculations successfully in a three-dimensional (3D) embedding lattice requires an optimal use of the symmetries of the model in order to keep the basis set of states to a practical size. In the Appendix we outline how we exploit the symmetries of the 3D lattice.

In the next section we describe the extension of the RD model and the corresponding master equation. We focus on two properties: the renewal time τ and the diffusion coefficient D, and determine them directly from the master operator. The renewal time is the time needed for the chain to assume a new configuration, which has no memory of the original one. It is found from the gap in the spectrum of the master operator. The master equation always has a trivial eigenvalue 0, corresponding to the stationary state. Any other initial state ultimately decays toward the stationary state, and the slowest relaxation time (the inverse of the gap) is the renewal time. The gap decays with a negative power z of the length N of the chain, such that $\tau \sim N^z$. The zero-field diffusion coefficient D is related to the drift velocity in a weak driving field and decays as a power N^{-x}. The approach to this asymptotic behavior is the main issue of this paper.

Due to the additional types of hopping, the dimensionality d of the embedding lattice plays a nontrivial role. We report calculations in $d=3$. They became possible through subtle use of the symmetries of the model, which are discussed in the Appendix. The subsequent sections contain the results for the renewal exponent z and the crossover functions, which describe the data for all lengths N, and the strengths of the transition rates for barrier crossing and hernia creation and annihilation. The results for the diffusion coefficient D and its exponent x are calculated from a linearization of the master equation with respect to the driving field. The exponents z and x are linked through the mean square displacement of the wandering chains. In the Discussion we comment on the results and explain why the crossover in gels is different from that in polymer melts.

Paessens and Schütz [9] have also extended the RD model by including "constraint release" in the hopping rates. In our language, this is a mix of hernia creation-annihilation and barrier crossings. We comment on their calculation in the discussion.

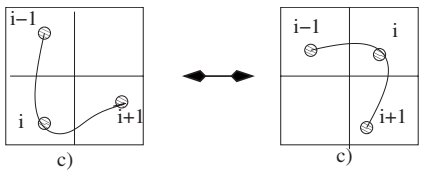

FIG. 2. Barrier crossings with hopping rate c.

Earlier [10] we performed a similar investigation for the cage model (in $d=2$), with similar conclusions as in the present study. Investigation of the RD model elucidates how far the crossover is model independent.

II. THE MODEL

The model consists of a chain of $N+1$ reptons located in the cells of a (hyper)cubic lattice. They are connected by N links, labeled by $\mathbf{Y}=(y_1,\ldots,y_N)$. The links take on the value $y_i=0$ (slack) or any of the 2D vectors that connect a cell to its neighbors (taut). The corners of the squares in $d=2$ or the edges of the cubes in $d=3$ are barriers for the chain. The reptons can move in three ways.

(1) The standard RD move, in which a repton between a slack and a taut link moves to the neighboring cell, thereby interchanging the slack and taut links. For these moves no barriers have to be overcome. A move is illustrated in Fig. 1. The strength of the hopping rate for RD moves sets the time scale and is therefore put equal to 1.

(2) The barrier crossings, of which an example is shown in Fig. 2. This is an interchange of two taut links connected to the same repton that jumps over the barrier. The strength of the transition rate for such a move is taken to be c.

(3) The creation of a hernia, which is a change in two consecutive slack links, from which the middle repton jumps to a neighboring cell. The annihilation is the reverse process. An example is shown in Fig. 3. Hernia creation and annihilation occur with the rate h.

The statistics of the model is governed by the master equation for the probability distribution $P(\mathbf{Y},t)$, where $\mathbf{Y}$ stands for the complete configuration $(y_1,\ldots,y_N)$. It has the general form

$$\frac{\partial P(\mathbf{Y},t)}{\partial t} = \sum_{\mathbf{Y}'} [W(\mathbf{Y}|\mathbf{Y}')P(\mathbf{Y}',t) - W(\mathbf{Y}'|\mathbf{Y})P(\mathbf{Y},t)] \equiv \sum_{\mathbf{Y}'} M(\mathbf{Y},\mathbf{Y}')P(\mathbf{Y}',t). \quad (1)$$

The W's are the transition rates of the possible motions that we have indicated in the above list. The matrix M combines the gain terms (in the off-diagonal elements) and the loss

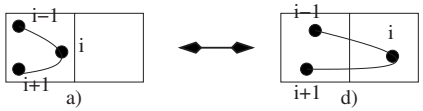

FIG. 3. Hernia creation (a)–(d) and annihilation (d)–(a). Both processes occur with rate are h.

terms (on the diagonal). M is the sum of matrices, one for each repton,

$$M(\mathbf{Y},\mathbf{Y}') = \sum_{i=0}^{N} M_i(\mathbf{Y},\mathbf{Y}'), \tag{2}$$

where the sum runs over the reptons starting with the tail repton $i=0$ to the head repton $i=N$. The internal reptons induce transitions between two configurations which differ in two consecutive y_i, the external (head and tail) reptons change only y_N and y_1. If we view the links as "bodies," the problem is equivalent to a one-dimensional many-body system with two-body interactions between nearest neighbors.

The matrix M is asymmetric because the transition rates are biased by a factor $B=\exp(\epsilon/2)$ for the moves in the direction of the field and by B^{-1} for the reverse process. ϵ is a dimensionless parameter representing the strength of the field. M is a stochastic matrix since the sum over each column vanishes. Therefore M has an eigenvalue 0 and the corresponding right eigenvector is the probability density of the stationary state. All other eigenvalues are negative. The smallest in magnitude is the gap, giving the slowest decay to the stationary state, and the inverse of the gap we take as the definition of the renewal time. The diffusion coefficient D is calculated from an infinitesimally small driving field. The field induces a drift v_d and via the Einstein relation

$$D = \frac{1}{N}\left(\frac{\partial v_d}{\partial \epsilon}\right)_{\epsilon=0} \tag{3}$$

the diffusion coefficient results. It is determined by expansion of the master equation in powers of ϵ,

$$\mathcal{M} = \mathcal{M}_0 + \epsilon\mathcal{M}_1 + \cdots, \quad P(\mathbf{Y}) = P_0(\mathbf{Y}) + \epsilon P_1(\mathbf{Y}) + \cdots, \tag{4}$$

which leads to the equations

$$\mathcal{M}_0 P_0 = 0, \quad \mathcal{M}_0 P_1 = -\mathcal{M}_1 P_0. \tag{5}$$

The first equation is trivially satisfied by a constant $P_0(\mathbf{Y})$, since the matrix M_0 is symmetric and the right eigenvector becomes equal to the trivial left eigenvector. The right-hand side of the second equation is a known function of the configuration. Thus it yields the linear perturbation P_1. The drift velocity is an average over the distribution [7]. The linear term in ϵ of the drift velocity involves the terms P_0 and P_1. With these terms we can calculate the linear term in v_d and find with (3) the diffusion coefficient D.

III. THE EXPONENT z FOR THE RENEWAL TIME

The easiest way to obtain the exponent of the relation $\tau = N^z$ is to make a log-log plot and determine the slope. In a previous publication [8], it was shown that this is rather misleading for the present problem. A much more sensitive check is to compute local exponents z_N according to

$$z_N = \frac{\ln \tau(N+1) - \ln \tau(N-1)}{\ln(N+1) - \ln(N-1)} \simeq \frac{d \ln \tau}{d \ln N}, \tag{6}$$

which gives z as a function of the chain length N. The function z_N is the basic ingredient for further analysis.

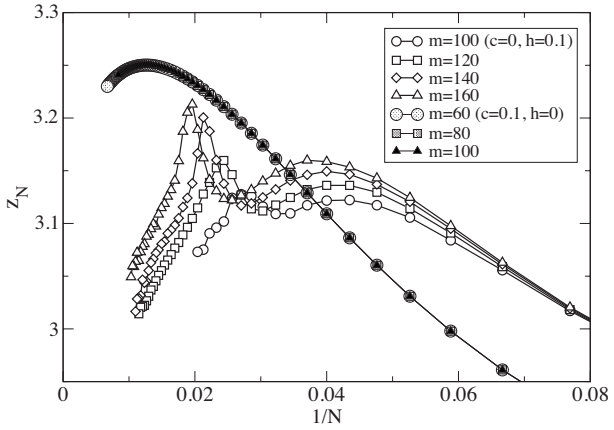

FIG. 4. Influence of the basis size m on the renewal time exponent for two combinations of parameters: $c=0$, $h=0.1$ and $c=0.1$, $h=0$.

First we check how accurately it can be obtained from a DMRG calculation of which the convergence is determined by the basis size m. In Fig. 4 we show examples of poor and excellent convergence. Poor convergence occurs for the combination $c=0$, $h=0.1$, where we have no barrier crossings but substantial hernia creation and annihilation. For a length $N=20$ the size of the basis, even as large as $m=160$, still has an influence, and for longer chains this becomes stronger. Thus it is difficult to deduce from these data the effective exponent for chains longer than $N=20$. In the second combination $c=0.1$, $h=0$, the convergence is perfect for much smaller bases and for much longer chains, as the upper curve in the picture demonstrates. In fact, the case with no barrier crossing at all is the only combination where convergence is a problem, as subsequent pictures will show. We blame the lack of convergence on the fact that hernia creation and annihilation without some barrier crossing leads to a large weight for configurations with many hernias and therefore to a short end-to-end distance of the chain. These are atypical configurations and the DMRG procedure has difficulty in finding an adequate basis to represent the gap state.

Some other noticeable points are as follows.

(1) The curves have still not reached the asymptotic value for values of N of the order of 100. Thus a log-log plot would suggest a higher value than the reptation value 3. This slow approach to the asymptotic value has been identified as the main reason for the discrepancy between the theoretical reptation exponent $z=3$ and the measured higher values [8]. We get a better grip on the asymptotics when we discuss the crossover.

(2) The curves do not indicate a tendency toward the Rouse exponent $z=2$. This illustrates the point made in the Introduction that the two mechanisms have to assist each other, before deviations from reptation occur.

Figure 5 shows a set of curves for $h=0$ and a set of values c. Note that the effective exponent is quite sensitive to the value of c, but all curves do not show reptative behavior, as was mentioned earlier for the N dependence of a single point in parameter space. For larger values of c, a maximum in the effective exponent z_N seems to develop for larger and larger N. As the maximum can easily be interpreted as a saturated

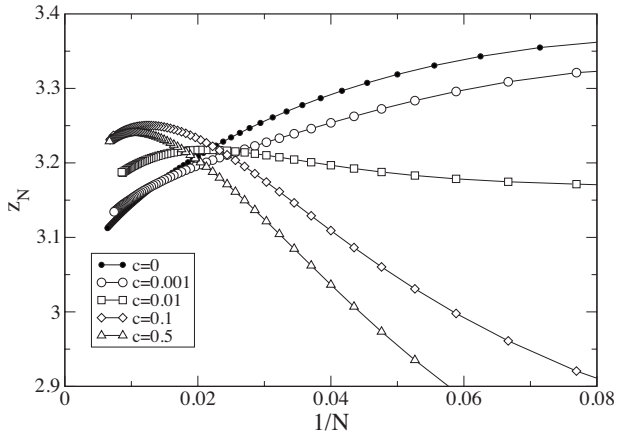

FIG. 5. Renewal time exponent z_N for $h=0$ and a set of values c.

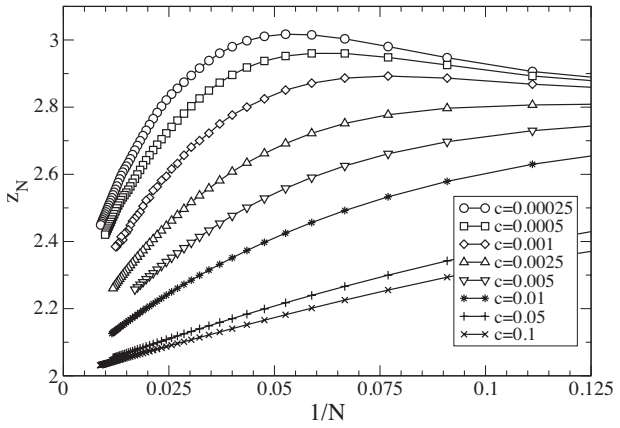

FIG. 7. Renewal time exponent z_N for $h=0.1$ and a set of values c.

asymptotic value in a log-log plot, these corrections to scaling, still present for very long chains, are very important for assessing the correct asymptotic behavior. This feature makes it necessary to do a finite-size analysis in order to get a grip on the region in N where the behavior changes.

The standard argument is that hernia creation and annihilation do not change the reptative character of the chain motion because they leave the backbone of the chain invariant; this is the collection of taut links after the chain has been successively stripped of its hernias. The backbone changes only by refreshment at the ends of the chain. Also, barrier crossing seems to be, as a single mechanism, ineffective. It changes the backbone, but not the number of taut links in a certain direction, since in a barrier crossing taut links are only interchanged in position along the chain. We may call the properties of the chain, which are not changed by internal motion, "quasi-invariants." So one needs both a nonzero c and a nonzero h to remove these quasi-invariants. The cooperation of hernia creation and annihilation and barrier crossing is an intricate mechanism. Therefore we concentrate first on the situation where one of them has a finite strength and the other becomes small.

IV. SIMPLE CROSSOVER

The case where one of the two, c or h, is fixed at a finite value gives a simple crossover from reptation to Rouse dynamics when the chain grows with N. As an example, consider first a fixed value $c=0.1$ and h varying and small, for which the local exponent z_N is given in Fig. 6. The reverse situation is plotted in Fig. 7 with z_N for $h=0.1$ and a set of values of c. The two figures are strikingly similar. For small values of the parameter c (h), the chain seems to show reptative behavior but turns over toward the Rouse exponent $z=2$ for longer chains. It is remarkable that even in Fig. 7 the values for very small c show this trend, while we know from the previous section that for $c=0$ the calculation is poorly convergent.

Anticipating the asymptotic values of the two regimes, the following representation is adequate for the renewal time (for fixed h):

$$\tau(N,c) = N^3 g(c^\theta N). \tag{7}$$

The idea is that all curves of, e.g., Fig. 7 are represented by a single curve $g(x)$. Thus we have plotted in Fig. 8 the data for τN^{-3} as a function of $c^\theta N$ for the fixed value $h=0.5$ and

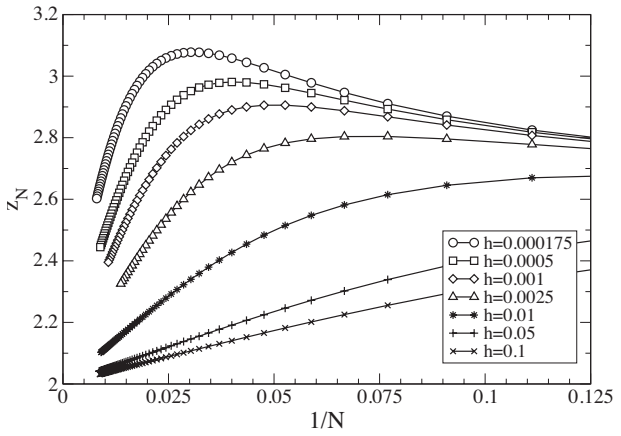

FIG. 6. Renewal time exponent z_N for $c=0.1$ and a set of values h.

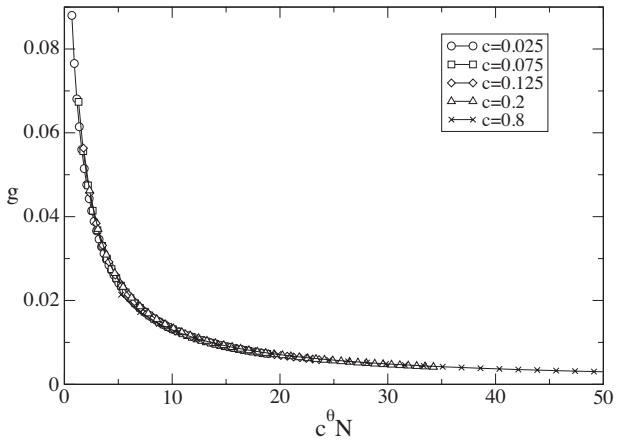

FIG. 8. Crossover scaling function $g(x)$ for $h=0.5$ and $\theta=0.58$.

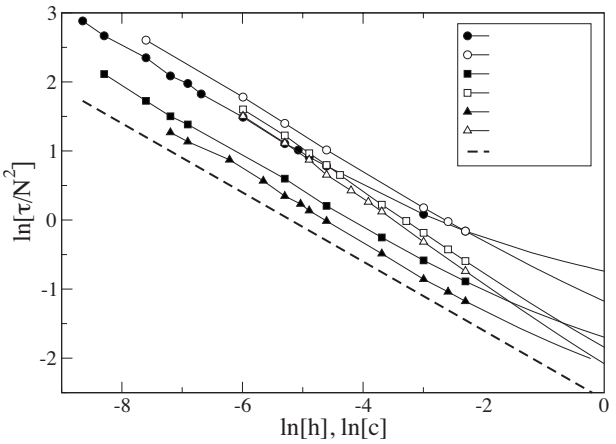

FIG. 9. Crossover exponent θ as deduced from (10). It is given by the slope of the curve.

varying c, with an assumed value $\theta=0.58$. This exponent is determined by trial and error to get the maximum collapse of the data on a single curve. The figure shows indeed a nice data collapse but it hides a subtlety which we can uncover by using the properties of the crossover function $g(x)$. The function $g(x)$ should be expandable for small arguments as

$$g(x) = g_0 + g_1 x + \cdots \tag{8}$$

and for large arguments as

$$g(x) \simeq \frac{1}{x}\left(g_{-1} + \frac{g_{-2}}{x} + \cdots\right). \tag{9}$$

Then τ varies as N^3 for vanishing c and as N^2 for $N\to\infty$ (at nonzero c). Inserting the asymptotic behavior (9) into (7), we obtain

$$\ln(\tau/N^2) = \ln g_{-1} - \theta \ln c + \cdots, \tag{10}$$

where the ellipsis refers to corrections of order $1/N$. In Fig. 9 we have made a plot of the limit of $\ln(\tau/N^2)$ vs $\ln c$. The values of the vertical axis are extrapolated to $N\to\infty$, which corresponds to the first two terms of (10). We first check whether the basis of states is large enough that we have no systematic errors due to a too small basis. Then we inspect whether τ/N^2 has a well-defined limiting value for $N\to\infty$. (The values should approach the limiting point in a fairly linear way.) If the curves in Fig. 9 have a straight slope, a well-defined value of the crossover exponent θ follows. As one observes, there rather is a constant slope for small values of c and another one for the larger values of c. Now crossover may only be expected in the limit of $c\to 0$, which gives a slope in the neighborhood of $\theta\simeq 0.5$. We could therefore discard the behavior for larger c, as not being described by crossover, but this contrasts with the findings for the cage model, where the crossover formula applies for practically the whole range of c. We show the data also for larger values of c because we find it intriguing that this region is also representable by a crossover function, albeit with a different crossover exponent.

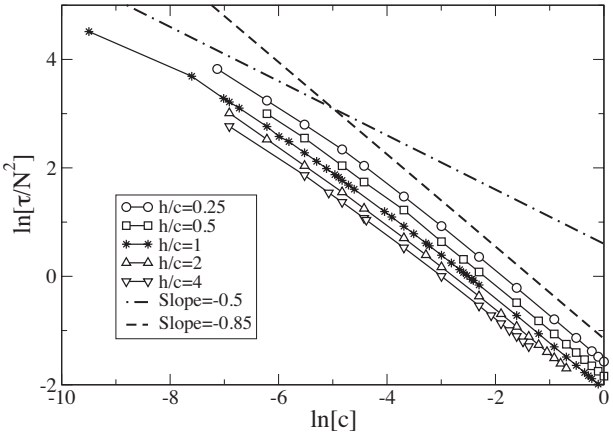

FIG. 10. Crossover exponent θ for ratios of h/c.

V. CROSSOVER ALONG LINES $h/c=r$

With one of the parameters h or c fixed, it is the other parameter that controls the crossover. The real challenge is to find a representation where both mechanisms feature. We have not been able to find a simple expression that accurately accounts for arbitrary combinations of h and c. We gain some insight into the combined action of h and c by approaching the limit $h=c=0$ along a radial line $h/c=r$. For fixed r we have again a single parameter which, in combination with N, provides a crossover scaling variable, such that we can use the scenario of the previous section to analyze the data. In Fig. 10 we give the crossover exponent θ as a function of $\ln c$ ($\ln h$) and for some values of the parameter ratio h/c. For very small values of $\ln c$ ($\ln h$) the slope of the line is compatible with the "universal" exponent $\theta=0.5$. However, for larger values another exponent seems to emerge of the order of $\theta=0.85$. Note that the curves in Fig. 10 run quite parallel, which means that r enters only in the offset given by g_{-1} in (10). To show this point in more detail we have plotted in Fig. 11 the lines for larger values of h (or c). The window where the large exponent $\theta=0.85$ applies covers more than an order of magnitude for a fixed ratio h/c.

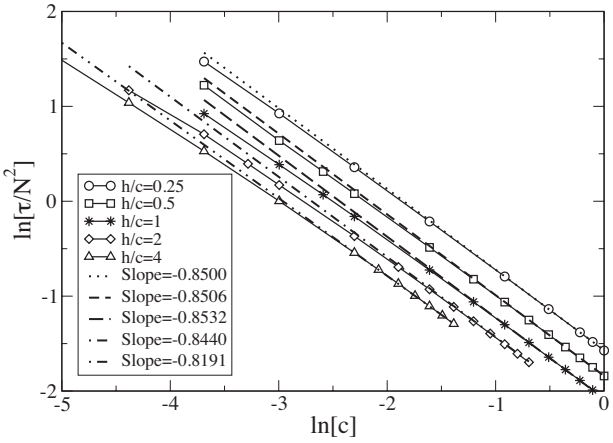

FIG. 11. Crossover exponent θ for ratios of h/c at larger values of h and c.

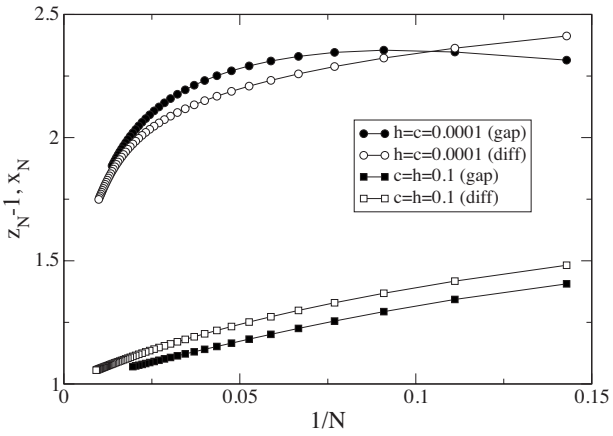

FIG. 12. Comparison of the exponents z_N-1 and x_N.

VI. THE DIFFUSION COEFFICIENT *D*

The diffusion coefficient has been determined by the linearization (5), which gives the linear response of the drift velocity with respect to the driving force. We do not repeat the analysis for the diffusion exponent x, since diffusion and renewal time are closely related. If the center of the chain has drifted over a distance of the order of the end-to-end distance $\sqrt{N}$, the chain has renewed itself. The mean square displacement due to diffusion during a renewal time equals $D\tau$. So one has the connection

$$D\tau \simeq N \quad \text{for } N \to \infty. \tag{11}$$

This relation implies the relation for the exponents $z-x=1$. We have tested this relation, and in Fig. 12 we show the values of z_N-1 and x_N for the same set of parameters, one for the small value $h=c=0.0001$, where the behavior is more reptative, and one for the larger value $h=c=0.1$, where the exponents tend to Rouse dynamics. See also Fig. 13, which shows that the crossover exponents θ for renewal and for diffusion are practically the same in the domain where they could be calculated with reasonable accuracy.

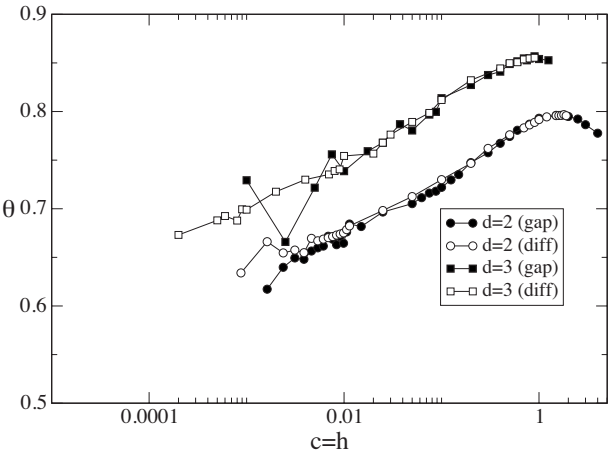

FIG. 13. Comparison of the crossover exponent θ for $d=2$ and $d=3$, for both the gap and the diffusion coefficient.

VII. TWO-DIMENSIONAL RESULTS

We have shown the results for embedding dimension $d=3$. As mentioned, the general expectation is that the embedding dimension has little influence on the universal properties. We are now in a position to verify this statement, since we have made extensive calculations in both $d=2$ and $d=3$. Indeed we come to the conclusion that the results agree qualitatively. To show an example we plot in Fig. 13 the $d=3$ and $d=2$ curves for θ for $h=c$. The trends are the same, but the value of θ in the "large" parameter regime is definitely larger for $d=3$ than for $d=2$.

VIII. DISCUSSION

As a follow-up to the study of crossover in the cage model, the extended RD model gives by and large the same picture: with growing length the chain crosses over from reptation to Rouse dynamics. The story is more complicated here because the two extra types of hopping, barrier crossing and hernia creation and annihilation, have to assist each other in order to obtain Rouse dynamics for long chains. This makes a comprehensive representation of the data in one scaling expression complicated. We have investigated the crossover behavior along lines in the c,h plane.

The underlying idea of crossover is that there are two competing time scales. One is the diffusive time scale N^2/D_c, which is the time needed for a perturbation to diffuse along the chain inward. We note that here not the overall diffusion D but the curvilinear diffusion coefficient D_c applies, which decays as N^{-1}. This time scale leads to a renewal time $\sim N^3$. The other time scale is the time needed to renew the chain by the combined action of hernia creation and annihilation and barrier crossing. If one of the parameters c or h is large enough, the other is the limiting factor. If c is the smaller one, the time scale due to c equals N/c and if h sets the rate, it is N/h. The fastest of the two time scales sets the overall rate and therefore crossover occurs when they are equal, i.e., when $c \sim N^{-2}$, or $h \sim N^{-2}$, whichever is the smaller parameter. This leads to a crossover exponent $\theta=1/2$. We see this trend in the numerical data, but the fact that we have to go to really small values of c (or h), and therefore to correspondingly large N, prevents this "universal" crossover exponent from showing up in a clear way.

On the other hand, we observe for larger values of the parameters crossover behavior also, with different crossover exponents θ. This change in value could be a demonstration of corrections to scaling, just as the exponents z_N or x_N are rather far from their asymptotic values when crossover plays no role (as, e.g., Fig. 5 shows). Clearly the renewal of the chain by sideways motion is still slow enough, even when c and h are of order unity, that the competition with diffusive renewal determines the character of the dynamics.

As pointed out earlier for the cage model [10], the crossover differs from the common scenario for polymer melts, where the crossover is in the opposite direction: from Rouse dynamics to reptation [11]. In the melt, reptation results for the longer chains because the restriction in motion of the

polymer, due to the presence of others, becomes more severe as the polymer gets longer. We have argued that such crossover in melts can be understood from sideways motions that have a rate depending on the length of the chain. If the renewal time is taken as indicative of the lifetime of a barrier, the sideways motion will have a rate $\sim N^{-z_N}$ in the melt. The combined scaling parameter cN^2 then will shrink as N grows. Since we always find $z_N > 2$, reptation prevails for long chains in the melt. One would have to do a self-consistent calculation, as carried out by Paessens and Schütz, to make this argument quantitative [9].

Paessens and Schütz [9] have also extended the RD model with rates that depend on the length of the chain. Their aim is to see the influence of "constraint release" on finite chains. The constraint release that they allow is in our language a mix of hernia creation and annihilation and barrier crossing. But not all types of barrier crossing that we allow are permitted in their model. So it is somewhat difficult to make a clear comparison between their findings and ours. The interesting point of their calculation is the requirement of self-consistency: the rates determine the renewal time and the renewal time in turn influences the rates. To carry out this program accurately within the DMRG method is one of the challenges for further research.

ACKNOWLEDGMENTS

The authors have benefited very much from many stimulating discussions with Gerard Barkema. A.D. thanks Wroclaw Centre for Networking and Computing for access to their computing facilities (Grant No. 82).

APPENDIX: THE SYMMETRIES OF THE MASTER OPERATOR

It is easy to set up a DMRG without paying attention to the symmetries of the problem. Then in $d=3$ each link can be in $2d+1=7$ states, leading to 7^N configurations for $N+1$ reptons. The possible symmetries in the problem will give an equal probability to many configurations. If the symmetries are not explicitly acknowledged, the symmetries get lost when the choice of basis states does not conserve the symmetry. This means that states which are equivalent by symmetry have to be chosen simultaneously. Thus either one has to include a large number of states, which leads to impractical calculations, or one has to keep track of the symmetry in each step of the method, which requires a substantial extra amount of careful programming. However, since we want to extract the utmost out of the data, we have no choice and must optimize the symmetry.

As we deal with a field-free gap for the renewal time and with the field-free equation (5), we can employ, in principle, the full symmetry group of the cube, which has 48 elements. If we were to do an exact calculation, we could apply all the relevant symmetry operations to the wave function and so reduce the number of components. But that is not the way the DMRG works. The configuration space is split into tail and head parts, and the wave function is improved by an optimal choice of basis states in one part using the density matrix induced by the other part. In order to keep the symmetry in the wave function, the chosen states have to have the symmetry, which implies that the density matrix must have the symmetry. That in turn implies that, in each stage of the calculation, the wave function of the whole chain must have the desired symmetry. Thus we have to know how to combine the symmetry of the parts in order to get the symmetry of the whole. This is similar to combining angular momenta of particles in atomic physics to get the angular momentum of the total wave function. The "good quantum numbers" are derived from a set of commuting symmetry operators.

We can find at most three commuting operators within the cubic group, with some freedom of choice. The simplest method would be to look to the reflection symmetry of the coordinate axes. For each of the three operations the wave function can be even or odd, giving eight sectors labeled by the parities. The parities qualify as good quantum numbers. The ground state (stationary state) is located in the sector that is even under all three reflections. Each of the other sectors contains an excited state, and the smallest (in magnitude) is the gap. The parities of the parts can easily be combined with each other for the total since they simply multiply. We have implemented this scheme, but it does not lead to very accurate results; we blame this on the rather unbalanced occupation of the sectors, when the most probable states of the density matrix are chosen.

The most successful use of the symmetry comes from another choice of commuting symmetry operations. We put the field in the direction of the body diagonal and consider rotations around this diagonal. We may rotate over the angles $\phi=0$, $2\pi/3$, or $4\pi/3$, leaving the problem invariant. Under a rotation the wave function is multiplied by a phase factor $\exp(i\phi)$, which qualifies also as a good quantum number, leading to three sectors. Rotations commute with simultaneous inversion of the coordinate axes, doubling each of the three rotation sectors. As the first three sectors we take those that are invariant under inversion, and the next three are odd under inversion. The ground state is in the first and the gap is in the fourth sector (invariant under rotation and odd under inversion). The advantage of these good quantum numbers is that we can combine the quantum numbers of parts (by simple multiplication) to give the same set of quantum numbers for the combination. For instance, a part in sector 2 ($\phi=2\pi/3$) and one in sector 3 ($\phi=4\pi/3$) lead to a combination with $\phi=0$, which is therefore in sector 1. This use of symmetry gives good results, but it is not yet optimal.

A refinement could be made by considering the interchange of the x and y axes. This turns the first and fourth sectors into themselves and transforms sectors 2 and 3 as well as 4 and 5 into each other. Although there is no good quantum number associated with this operation, we could use this symmetry by splitting sectors 1 and 4 into even and odd parts under the interchange. This leads to eight "channels," which partly coincide with the previous sectors. Combining a part in sector (channel) 2 with a part in 3 does give an overall state in sector 1, but one has to take even and odd combinations to get them in the even and odd channels cor-

responding to sector 1. This gives a substantial amount of extra programming in order to properly keep track of the channels. But the effort is rewarded, as it improves the accuracy, which is needed for the delicate cases of the parameter space. This choice of sectors (channels) is efficient because the states of the density matrix, which are chosen as having the largest eigenvalues, are more or less evenly distributed over the channels.

[1] P. G. de Gennes, J. Chem. Phys. **55**, 572 (1971); *Scaling Concepts in Polymer Physics* (Cornell University Press, Ithaca, NY, 1971).
[2] M. Rubinstein, Phys. Rev. Lett. **59**, 1946 (1987).
[3] T. A. J. Duke, Phys. Rev. Lett. **62**, 2877 (1989).
[4] M. Doi and S. F. Edwards, *The Theory of Polymer Dynamics* (Oxford University Press, New York, 1989).
[5] J. L. Viovy, Rev. Mod. Phys. **72**, 813 (2000); S. R. White, Phys. Rev. Lett. **69**, 2863 (1992).
[6] U. Schollwöck, Rev. Mod. Phys. **77**, 259 (2005).
[7] B. Widom, J.-L. Viovy, and A. D. Defontaines, J. Phys. I **1**, 1759 (1991).
[8] E. Carlon, A. Drzewiński, and J. M. J. van Leeuwen, Phys. Rev. E **64**, 010801(R) (2001).
[9] M. Paessens and G. M. Schütz, Phys. Rev. E **66**, 021806 (2002).
[10] A. Drzewiński and J. M. J. van Leeuwen, Phys. Rev. E **74**, 061801 (2006).
[11] Kurt Kremer, Gary S. Grest, and I. Carmesin, Phys. Rev. Lett. **61**, 566 (1988); A. Wischnewski, M. Monkenbusch, L. Willner, D. Richter, and G. Kali, *ibid.* **90**, 058302 (2003).